

DMiCE – a depth-of-interaction detector design for PET scanners.

T.K. Lewellen, Senior Member IEEE, M. Janes, R.S. Miyaoka, Member IEEE,
University of Washington Medical Center, Seattle, WA.

Abstract--We have previously reported on a depth-of-interaction (DOI) detector design that uses light sharing and a single-ended readout scheme. The approach depends on the modification of light transmission between paired crystals to produce a DOI effect when the ratio of the light emitted by the paired crystals was measured. A limitation of the design was the method used to control the light sharing – making production of detector modules a complicated and time consuming task. We report here on the use of laser cut reflector sheets placed between paired crystals as an efficient method to construct such modules. Simulations of 4x4 and 1x1 mm cross section crystals were performed. The simulation results indicate that a triangular reflector shape between the crystals and an air-gap reflector design around the crystals provides the best performance. The optimal length of the reflector (% length of crystal) is a function of the crystal cross section and varies between 100% for a 4x4x30 mm crystal pair to 73% for a 1x1x30 mm crystal pair. Initial experimental validation of the simulations is being done with hand cut reflector patterns with 4x4x30 mm crystals. The work will then progress to using laser cut patterns laminated between slabs of crystals, which are then cut into crystal pairs for mounting on PMTs.

I. INTRODUCTION

We have previously reported on a depth-of-interaction (DOI) detector design that uses light sharing and a single-ended readout scheme [1]. The motivation of the initial development was to produce a cost effective DOI system that could be adapted to a wide variety of crystal types since it did not rely on mixing of crystals with different characteristics such as is done in techniques using pulse shape discrimination. The use of a single photoreceptor (e.g. photomultiplier or APD) should result in a cost effective system in that the number of photoreceptors and associated electronic channels are minimized. Finally, a single ended approach also simplifies construction in terms of not having to accommodate signal paths and support of active devices on both sides of the crystal arrays. There were two major limitations in our approach. First, the design of the interface was a tedious process and because all of the application of paint was done by hand uniformity of fabrication was a concern. Second, the resulting DOI information was not as precise as has been achieved with double ended approaches.

We expect that the precision limitation can be partially compensated for with the inclusion of an appropriate model for detector response in the image reconstruction algorithm. While we have yet to implement DOI in such models, we have had success with detector response modeling due to crystal scatter and penetration [2]. The work reported on here is focused on overcoming the first limitation – the problem of a practical design that could be easily implemented for construction of a small animal PET scanner. We are faced with two conflicting requirements.

To improve the statistics, we wish to collect as much light as possible from each event. This requirement leads us to optimize the reflection properties of the design to “pipe” as much light as possible to the photoreceptor. The second requirement is to control the light sharing between the crystals to provide the DOI index and reduce the possibility of light crossing back over the shared optical interface after reflection (which decreases the precision of the DOI measurement). We have begun our investigation into solutions with simulations, but we recognize that our current surface models for both the crystal and the reflector between the shared optical interface are not realistic enough. Thus, the simulations are being used to define a basic design approach that then must be refined with systematic experiments with DOI detector units. We do plan to develop more accurate simulations (using our experimental data for validation) to pursue a more rigorous optimization study.

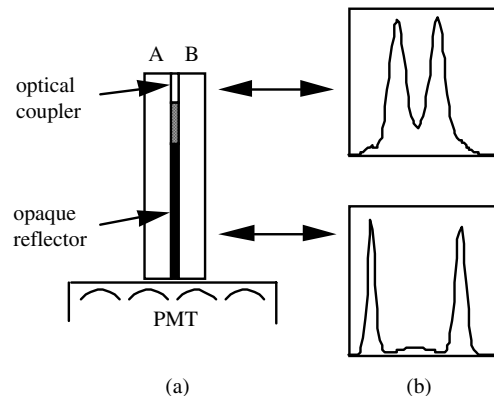


Figure 1. dMiCE detector concept. (a) DOI detector unit. (b) PMT ratio plots $[A/(A+B)]$. A significant amount of light is shared when an event is detected near the entrance face of the detector unit. Less sharing occurs for interactions near the PMT interface

II. MATERIAL AND METHODS

The design, termed dMiCE, builds upon our earlier work on the micro-crystal element detector module (MiCE) [3-5]. The basic approach for the DOI function is shown in Figure 1. The light sharing along the long length of a pair of crystals is used to create a DOI dependence on the ratio of the light outputs from the crystals $[A/(A+B)]$. The approach we have used is to allow no sharing near the PMT and full sharing near the front of the crystals (as shown in Figure 1). For our initial work, we utilized a multi-cathode PMT so that each crystal was directly coupled to a single photocathode. Our new approach is to use the same 3M polymer reflective film that we have used in our MiCE2 detector design [5] or other material such as aluminum. We envision laser-cutting patterns in to sheets of the reflector, and then laminating the reflector between slabs of crystal. The laminated slabs will then be cut into crystal pairs and

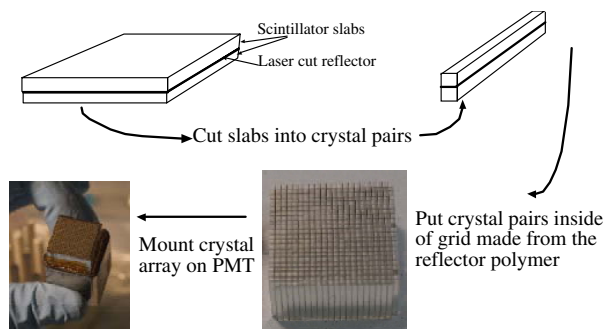


Figure 2: Basic approach to building the DOI module. Laminate laser cut reflector and crystal “slabs” then cut and polish the slabs into crystal pairs. Finally, put crystal pairs into grid of reflector polymer and mount on a PMT.

assembled onto the PMTs using a polymer reflective grid similar to that used for the MiCE2 design (Figure 2).

Our first set of experiments includes trials of the polymer reflector and aluminum foil. The inclusion of aluminum foil is a first step in exploring tradeoffs between the reflective properties of the materials used in the shared interface. We selected aluminum foil since it can be laser cut in the same manner as we have used for the polymer reflective film.

The first step in the investigation was a series of simulations carried out using the DETECT light transport modeling code. Crystal 30 mm long with 4 and 1 mm cross sections were explored. Surface treatments included polished and unpolished. In addition to the reflector shape between crystals, the use of laminated or an air-gap reflector around the outside of the crystal pairs was also investigated. The shapes investigated included rectangular strips of different widths and lengths, and triangular strips of different lengths.

Based on the simulation results, we began our experimental investigation with 4x4x30 LFS crystals and triangular reflectors. The crystals were initially polished and then the shared interface surface roughened. For these initial data, the degree of roughness was not measured nor carefully controlled - a step that we will implement as we proceed with more detailed experiments. The polymer and aluminum foils were hand cut into the desired shapes and then laminated between the crystal pairs with Meltmount 1.704 by Cargille. The crystal pairs were then mounted on a Hamamatsu R7600 16 channel, multi-anode PMT. The crystal pairs were carefully mounted so that each crystal was directly over one of the photocathode “pads” of the PMT. For the measurements, a point source as used in coincidence with the crystal pair under test and a 4x4x10 LFS crystal mounted on a Hamamatsu R2649 PMT. The crystal pair PMT was mounted on a linear stage and oriented so that the photon beam has normal to the long axis of the crystal pair (Figure 3). The PMT outputs from the R7600 were connected to an Ortec 855 dual spectroscopy amplifier operating with a time constant of 0.50 μ sec. The R7600 PMT outputs were also connected to an Ortec model CF2000 octal constant fraction discriminator module (CFD). The R2649 PMT was connected to a third channel of the CFD. The two CFD channels for the crystal pair signals were then summed together with an Ortec CO4020 quad

logic unit. The output of this unit was used as the stop signal to a Tenelec TC861A time to amplitude converter (TAC). The output for the R2649 was used as the TAC start signal. A Tenelec fast delay module (not shown in Figure 3) was inserted on the stop signal side to adjust the timing peak position in the TAC spectrum. The TAC output was processed by a Tenelec 451 timing SCA with the window positioned to include the full prompt peak in the TAC spectrum. The SCA output was used to gate an Ortec AD811 CAMAC analog to digital converter (ADC) that also processed the outputs from the two spectroscopy amplifier channels (i.e., the paired crystal signals). The data were collected with a Macintosh computer using a set of tools written in Labview (National Instruments, Austin, Tx) for controlling and processing data from our CAMAC system.

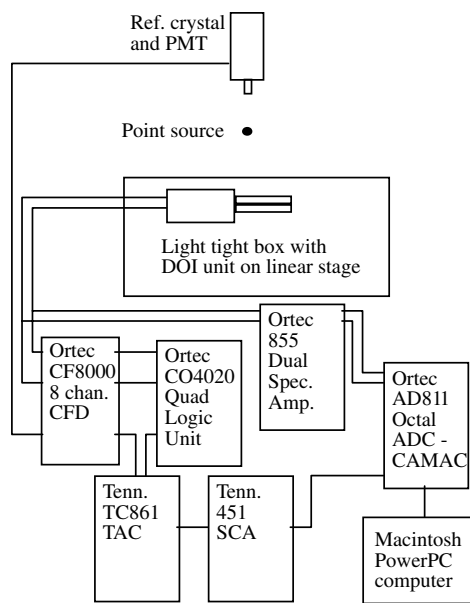


Figure 3: Block diagram of data acquisition electronics for DOI test module

III. RESULTS

The simulations of using a mirror reflector cut into different shapes to control the light sharing was done for 4x4x30 mm crystals. This size was selected for two reasons: 1) the initial experiments with real crystals will be this size to allow easier fabrication (by hand) of the reflector shapes; and 2) we wish to explore this approach to DOI for both small animal applications (crystal cross sections < 2x2 mm) and high resolution human systems (crystal cross sections of ~ 4x4 mm). The best results were obtained using unpolished surfaces on the light sharing interface with polished surfaces and an air gap reflector on the surrounding surfaces. The simulations also showed that the best shape for the reflector between shared crystals is a simple triangle. Examples of simulation runs for the 4x4 cross section crystals are shown in Figure 4. Figure 5 is a plot of the simulated ratio for the 4x4x30 crystal with a full triangular reflector, but for the light emission set on the center line of the crystal (set 1) and at 1 mm offset from the center line (set 2) indicating that we should not have a major problem with where in the cross section of the crystal the light

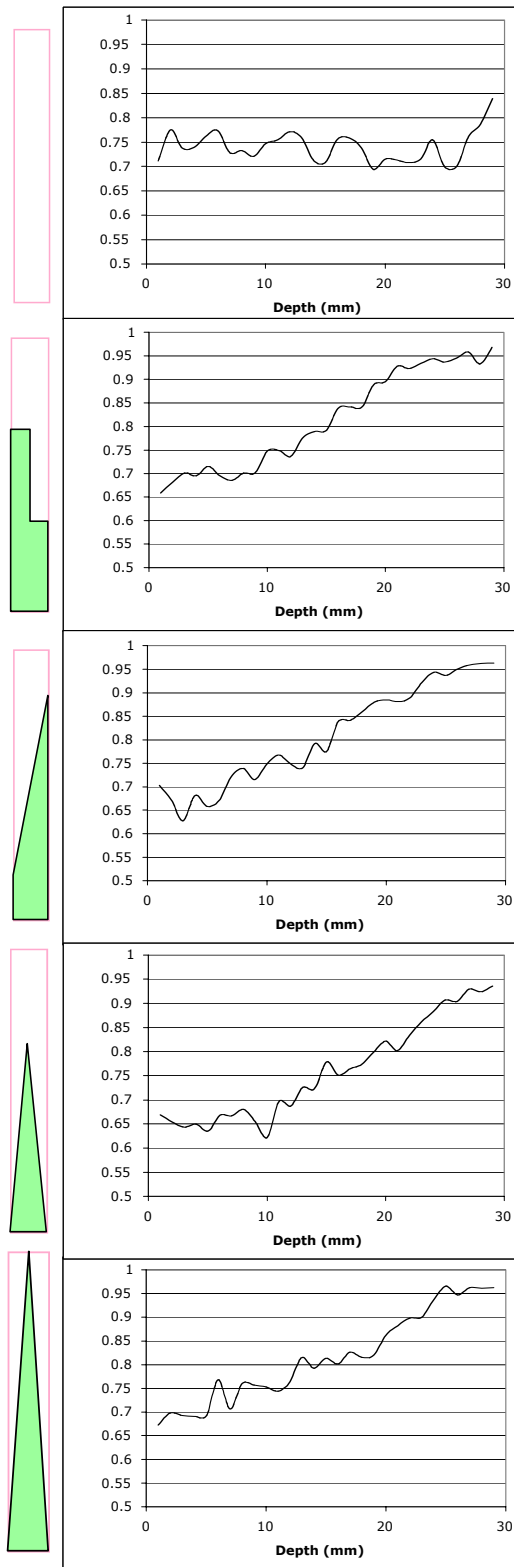


Figure 4: Examples of simulations of 4x4x30 crystals with different shapes of reflector between the crystals (top to bottom, no reflector, step, slant, small triangle, full triangle). The full triangle provided the most linear response.

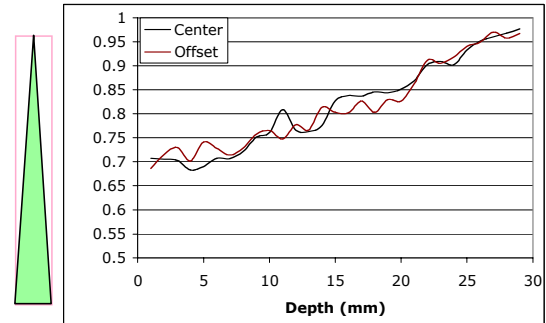


Figure 5: Ratio simulation for a 4x4x30 crystal with a full triangle reflector between the shared optical interface. Center is for the light emission point on the centerline of the crystal; offset is for the light emission offset by 1 mm from the centerline.

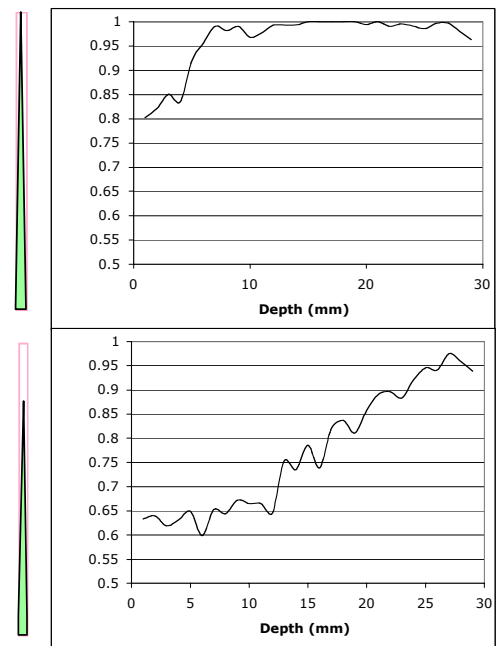


Figure 6: Examples of simulation results for a 1x1x30 mm crystal for a full triangle reflector (top) and a triangular reflector with length equal to 73% of the crystal length (bottom). The depth is mm from the front of the PMT.

emission occurs. For a 4x4x30 mm crystal, the triangle should be 30 mm long. However, when we simulated a 1x1x30 mm crystal, we found that the optimal shape was still a triangle but with the length equal to 73% of the crystal length (Figure 6).

Our initial experimental data were taken with 4x4x30 mm LFS crystals using triangular shapes cut from the 0.7 mm thick 3M mirror film or 0.0127 mm thick aluminum foil. In all cases, the crystals were wrapped in Teflon. The surfaces were either polished, unpolished, or polish surfaces that were then sanded. The conditions for the data reported here are listed in Table I. We found that the shapes had to be modified from our simulations to begin to get an approximate linear ratio versus depth response. Altering the reflectivity of the system (e.g., by sanding the surfaces

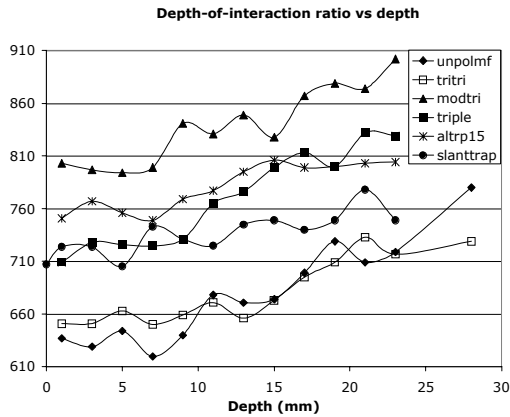


Figure 7: Plot of the DOI ratio versus depth for different reflector types and surface treatments. Depth is measured from the front of the crystal (PMT is at depth 30). Legends are defined in Table I.

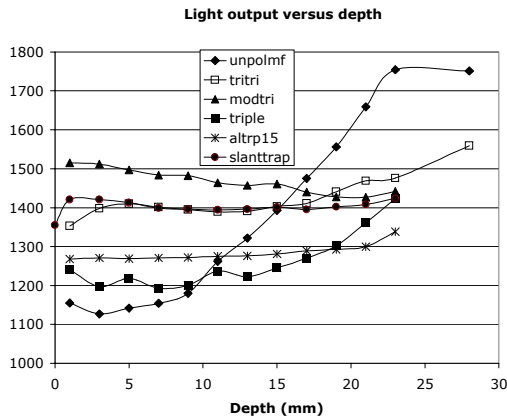


Figure 8: Plot of the total energy photopeak position (channel) versus depth for different reflector shapes and surface treatments. The depth is the distance from the end of the crystal (PMT is at depth 30). The legends are defined in Table I.

parallel to the interface) improved linearity. Using a less efficient reflector decreased the widths of the ratio distribution for any given depth. Figure 7 is a summary of the measured ratios for a series of different combinations of surface treatments and reflector types/shapes with the 4x4x30 mm crystals. Figure 8 is a plot of the total light output (PMT A + PMT B) for the data in Figure 8. Table I defines the legend abbreviations of Figures 7 and 8. The results show that we can tailor the linearity of response by changing the shape of the reflector on the shared light interface (Figure 7). In addition, as one would expect, using unpolished crystals results in a strong depth dependence on the total light collected (Figure 8). However, the width of the DOI index peaks for any single position is large as indicated in Figure 9 where we have plotted some example ratio plots with error bars indicating the half maximum points of the ratio distributions for each depth. While these data indicate a significant loss of precision as compared to our earlier work [1], this preliminary data set also indicates that the precision is a function of the reflector type (Figure 9).

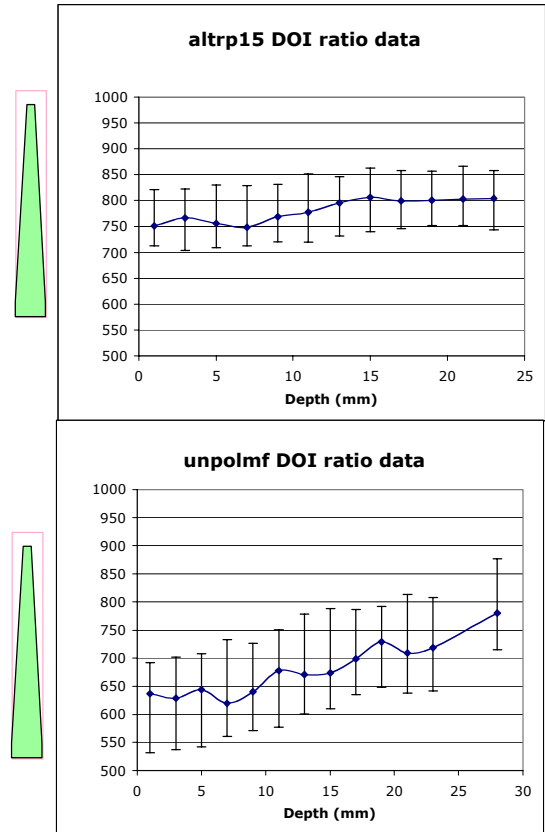


Figure 9: Plots of DOI ratio (line) and half maximum points of the DOI distribution (bars) versus depth. Depth is measured from the end of the crystal (PMT is at depth 30). The top plot is for altrp15 as defined in Table I and the bottom plot is for unpolmf (Table I).

IV. DISCUSSION

Our initial focus for the work reported here is development of the basic fabrication techniques and optimization of the light sharing techniques for our dMiCE detector design. The simulations were encouraging in that they show that relatively simple reflector shapes on the light-sharing interface can produce a linear response of the ratio to depth of interaction. However, a limitation of our simulations is that we do not have a good surface model for either the crystals or the reflectors. As a result, we have not pursued more in-depth investigations of variance or optimization via simulation. To evaluate our current simulations, we constructed several crystal pairs using reflector shapes as indicated by simulation made from the aluminum and 3M mirror film reflectors. The results obtained so far indicate that the trends in shape designs we found in our simulations carry over to measured data. The exact shapes were found to be different for the most linear responses, but more importantly, the precision of measurement was not as good as we had achieved with painted reflectors and absorbers on 2x2 mm cross section crystals [1]. The data obtained thus far leads us to hypothesize that the major problem in our precision of measurement is that there is too much light re-crossing the shared optical interface due to reflections. Increasing the

ratio slope would also be useful and that may well be possible with different shapes and types of reflectors. Thus, our future directions will include a careful study of methods to better control the optical interface and the amount of internal reflection in the crystal pair. In particular, careful attention to the surface treatment of all faces of each crystal to randomize the internal reflections coupled with careful design of the reflector/absorbers may well improve performance. It may also be that using an airbrushed paint template rather than metallic reflectors may allow us to further refine the internal reflection characteristics. We also expect that reducing the crystal cross section (e.g., from 4x4 mm to 2x2 mm) will have a major impact. Based on our previous work [1], we expect improved precision of measurement with the smaller crystals but that our designs will require different optimizations of the shared optical interface. As part of this effort, we will attempt to incorporate better surface models into our simulations so that we can explore optimization options with more powerful numeric tools.

The data to date have all been evaluated using a simple ratio to determine the DOI index. When the crystal pairs are assembled into modules, the interpretation of the data will be further complicated by scattering within the module. We will continue to use the ratio approach for optimizing the physical parameters of crystal pairs (reflector type and shape, crystal surface treatment). However, as we move on to develop full modules it is our expectation that best results will be obtained by implementing maximum likelihood estimators that include models of the light collection statistics, reflection of light photons back across the shared interface, and scattering within the module. One of the challenges of such an approach will be developing detector fabrication techniques that will provide a high degree of uniform performance from the crystal pairs in a module. Finally, we will also extend our pragmatic reconstruction algorithm detector modeling implementation [2] to include a model of the DOI performance of our module designs.

Our ultimate goal in this work is to demonstrate the feasibility and optimization of a single-ended readout implementation of a DOI module (dMiCE) for 4x4, 2x2, and 1x1 mm crystal cross sections. If successful, we plan to upgrade our MiCES scanner with such modules to increase

mm) may also provide proof of principle of this single ended approach for possible use in human sized scanners.

V. REFERENCES

1. Miyaoka, R., T. Lewellen, H. Yu, and D. McDaniel, *Design of a depth of interaction (DOI) PET detector module*. IEEE Trans. Nucl. Sci., 1998. **45**(3): p. 1069-1073.
2. Lee, K., P. Kinahan, J. Fessler, R. Miyaoka, and T. Lewellen. *Pragmatic Image Reconstruction for the MiCES Fully-3D Mouse Imaging PET Scanner*. in *IEEE Nuclear Science Symposium and Medical Imaging Conference*. 2003. Portland, OR.: IEEE p. in press.
3. Miyaoka, R., C. Laymon, M. Janes, K. Lee, P. Kinahan, and T. Lewellen. *Recent progress in the development of a micro crystal element (MiCE) PET system*. in *2002 IEEE Nuclear Science Symposium and Medical Imaging Conference*. 2002. Norfolk p. 1287-1291.
4. Miyaoka, R., S. Kohlmyer, and T. Lewellen, *A second generation micro crystal element (MiCE2) detector*. J. Nucl. Med., 2001: p. 110P.
5. Miyaoka, R., S. Kohlmyer, J. Joung, and T. Lewellen. *Performance Characteristics of a Second Generation Micro Crystal Element (MiCE2) Detector*. in *IEEE Nuclear Science Symposium and Medical Imaging Conference*. 2001. San Diego: IEEE p. 1124-7.
6. Miyaoka, R., M. Janes, B. Park, K. Lee, P. Kinahan, and T. Lewellen. *Toward the Development of a Micro Crystal Element Scanner (MiCES): quickPET II*. in *IEEE Nuclear Science Symposium and Medical Imaging Conference*. 2003. Portland, OR: IEEE p. in press.
7. Miyaoka, R., M. Janes, and T. Lewellen. *Optimization of Mounting Large Crystal Arrays to Photomultiplier Tubes*. in *IEEE Nuclear Science Symposium and Medical Imaging Conference*. 2003. Portland, OR.: IEEE p. in press.
8. Lewellen, T., R. Miyaoka, M. Janes, B. Park, and P. Kinahan. *System Electronics for the MiCES Small Animal PET Scanner*. in *IEEE Nuclear Science Symposium and Medical Imaging Conference*. 2003. Portland, Or. p. in press.

Table I: Legend definitions for Figures 7 – 9

Table of reflector types and shapes and crystal surface treatments. Meltmount 1.704 glue was used unless otherwise noted.

Legend	Shared interface	Unshared sides	Reflector type	Reflector shape
altrp15	sanded600 grit	polished	aluminum foil, and Meltmount 1.539 glue	28mm trapezoid, 1mm wide, atop a 2mm base
unpolmf	unpolished	unpolished	3m mirror film	28mm trapezoid, 1mm wide, atop a 2mm base
slanttrap	sanded 600 grit	polished	aluminum foil	28mm trapezoid, 1mm wide, atop a 2mm base
triple	sanded 320 grit	sides ll to interface are sanded 320 grit, others are polished	aluminum foil	28mm trapezoid, 1mm wide, atop a 2mm base
modtri	sanded 600 grit	polished	aluminum foil	25mm long triangle atop 3mm base
tritri	sanded 320 grit	sides ll to interface are sanded 320 grit, others are polished	aluminum foil	25mm long triangle atop 3mm base

the sensitivity without loss of spatial resolution of the system. The work with the larger crystals (e.g., 4x4x30